Experiments on Energy Redistribution by Thermal Radiation in Cylindrical Cavities

C. Stöckl and G. D. Tsakiris
Max-Planck-Institut für Quantenoptik, D-8046 Garching, Federal Republic of Germany
(Received 15 September 1992)

Experiments are presented that demonstrate the process leading to isotropization of the radiation field in a cavity heated by thermal x rays. Gold, cylindrical cavities 500 μm in diameter were heated from one side by $\simeq$154 eV thermal radiation from a laser plasma. The effect of the reemission in transporting energy along the cylinder axis was ascertained by comparing the axial temperature profile of "open" and "closed" geometry targets. The results are in good agreement with a theoretical model for the redistribution of energy via absorption and reemission of thermal radiation.

PACS numbers: 52.50.Jm, 44.40.+a, 47.70.Mc

The success of inertial confinement fusion (ICF) depends crucially on the degree of uniformity that a spherical capsule containing the nuclear fuel can be irradiated and subsequently imploded. Detailed studies [1,2] have shown that an irradiation uniformity of $\sim$(1–2)% is required for an instability-free implosion. In the direct drive approach to ICF a great deal of effort is devoted to develop techniques with which the required degree of uniformity can be achieved [3–5]. In the approach of the indirect drive [6], the capsule is positioned inside a high-Z cavity ("holhlraum") which is heated by x rays produced by lasers or ion beams. This latter scheme offers better symmetry characteristics due to the fact that the x-ray radiation is confined in the cavity and continuously interacts with the cavity wall. The multiple absorption and reemission process is then responsible for the isotropization of the radiation field and for the reduction of the temperature variation on the cavity wall. Furthermore, the capsule inside the cavity is irradiated with incoherent radiation.

When no sinks are present, a well insulated cavity heated for a prolonged time interval approaches asymptotically the equilibrium state where all the wall elements in the cavity have the same temperature despite the fact that the source irradiates the interior anisotropically [7]. What is of interest is the transitional period during which different wall elements possess different temperatures. In the more realistic case that sinks are present (e.g., open sections on the cavity wall or absorbing capsule in the cavity), the equilibrium state is not necessarily the one where a uniform temperature is established. Different sections of the cavity wall will, in general, possess different temperatures. It follows that, in connection with the design of a cavity for ICF purposes, it is important to know how fast the equilibrium state is approached and how it depends on such factors as cavity geometry, source power, and wall material. Also, in an optimization study it is of pivotal importance to be able to calculate the transient as well as the final temperature distribution in a cavity of a given geometry so that an estimate can be made of the energy required to achieve a certain degree of symmetry in x-ray irradiation of capsules.

In a recent publication [8] a theoretical model is described that can be used to calculate the spatial temperature variation and its temporal evolution on the wall of an arbitrarily shaped cavity heated by a source of x-ray radiation. It is based on the self-similar solution to the space- and time-dependent planar hydrodynamic equations with radiative heat conduction [9]. Experiments to date have been performed on spherical cavities and have dealt primarily with the study of the radiation confinement in a cavity [10–13]. In all of these experiments it was tacitly assumed that there is no temperature variation over the inner cavity surface so that the heating process could be described by a global temperature characterizing the cavity. Because of technical constraints, in a realistic situation the ICF cavity will be most likely nonspherical. Since in an arbitrarily shaped cavity the irradiation symmetrization of the capsule relies on the mechanism of absorption and reemission and the resulting energy redistribution, it is important to study this process in detail.

We report here the first experimental observation of the process on which the concept of the indirect drive is based, i.e., the temporal and spatial energy redistribution by thermal radiation. This process is manifested as an enhanced energy transport along the axis of a one-sided heated cylindrical cavity. The cylindrical geometry was chosen because it can be easily analyzed using the theoretical model in Ref. [8]. In addition, it appears to be a well suited geometry to the existing high power laser systems that are used in the ongoing ICF studies [14,15]. The experimental arrangement and the targets employed are shown schematically in Fig. 1. The target comprises two parts: the x-ray source consisting of a 500 μm diameter and 1 mm long cylindrical section with a 1100 Å thick Au foil on one side and the cylindrical cavity attached to it with the same diameter as the source but 10 mm long. The two types of cavities (open and closed geometries) were made by electroplating a 500 μm copper wire with a 10 μm layer of gold. Using photolithographic techniques, the 100 μm diagnostic slit was etched on the gold layer and in addition, in the open geometry target, most of the cylindrical wall ($\simeq$75%) was removed [see Fig. 1(b)]. The copper wire was finally

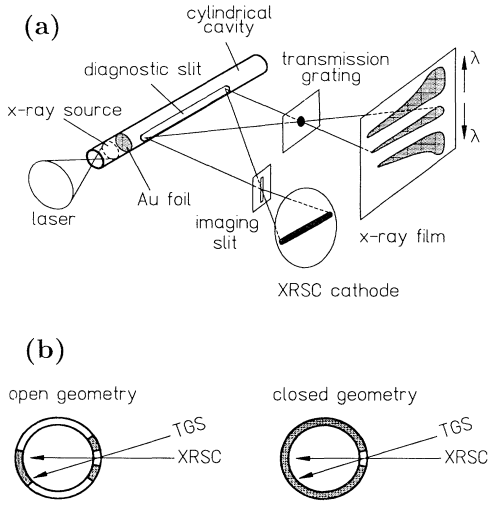

FIG. 1. (a) Schematic diagram showing the experimental arrangement and the targets (not to scale) and (b) cross-sectional view of the two types of cylindrical cavities. The viewing direction of the x-ray streak camera (XRSC) and that of the transmission grating (TGS) were both in the perpendicular plane to the laser and cavity axis. The XRSC was positioned in the horizontal plane and the TGS at an 18° angle above it.

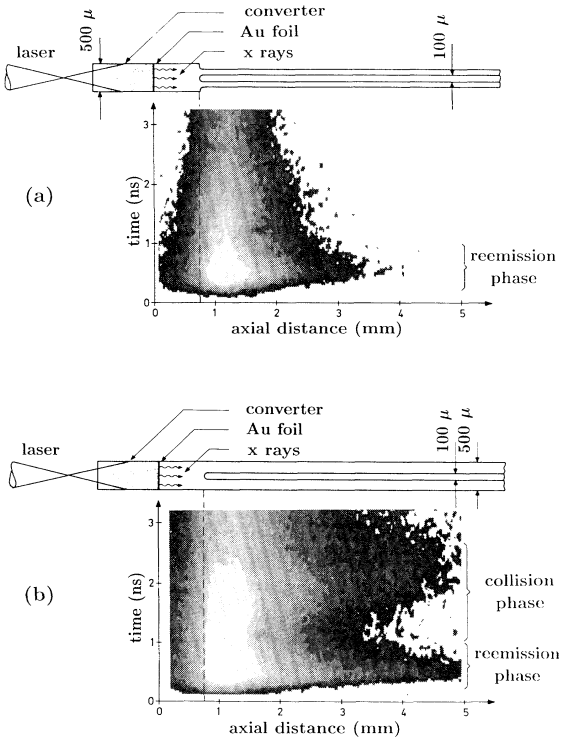

FIG. 2. Isointensity representation of the temporal evolution of the radiation emanating from the diagnostic slit of the (a) open and (b) closed geometry targets.

leached out. The total laser energy injected into the converter section was 200 J of $\lambda = 0.44$ μm (3ω) laser light from the ASTERIX IV iodine laser [16] having a pulse duration of 300 ps. The laser beam was focused at the entrance plane of the converter section so that part of the cylindrical surface as well as the foil were irradiated. A spatially resolving transmission grating spectrometer (TGS) utilizing absolutely calibrated Kodak-101 x-ray film as the detector [17] recorded the time integrated spectrum from each axial location of the diagnostic slit. A soft-x-ray streak camera (XRSC) [18] with an imaging slit (temporal resolution $\simeq$34 ps) measured the spectrally integrated flux along the slit with spatial resolution. The XRSC data from a representative shot with an open and a closed cylindrical cavity target are shown in Fig. 2. The source itself was carefully characterized [19] and it was found to deliver a nearly Planckian spectrum with $\simeq$154 eV radiation temperature having an x-ray pulse duration of $\simeq$700 ps and a one-sided laser to x-ray conversion efficiency of $\simeq$42%. The thickness of the Au foil between source and cylindrical cavity was determined so that less than 1% of the incident laser light is transmitted through it. The increase in pulse duration and x-ray conversion efficiency compared to a planar thin foil converter [20] is attributed to the collision at the axis of plasma from the cylindrical surface of the source [21].

The thermal radiation from the source was used to irradiate the interior surface of open and closed geometry targets from one side in the way indicated in Figs. 1 and 2. The measured flux emanating from the diagnostic slit temporally and spatially resolved is shown in Fig. 2. For the case of the closed geometry target [Fig. 2(b)], one can distinguish two phases in the temporal history of the emission. The reemission phase has approximately the duration of the x-ray source and it occurs during the time that the cylindrical cavity is empty, i.e., when the x-ray produced plasma is still confined at distances from the wall that are small compared with the radius of the cavity. It is followed after $\simeq$1 ns by the collision phase during which the wall plasma expands and subsequently implodes towards the axis of the cylinder. There, the kinetic energy of the expansion is converted back into thermal energy resulting in a new burst of x-ray emission [21]. The open geometry target [Fig. 2(a)] is seen to lack the collision phase. Also, the extent of the axial distance heated is smaller compared to the closed geometry target. Both effects are to be expected since most of the cylindrical surface is missing in this case. It should be noted here that the delay time between the two phases increases with the diameter of the cylindrical cavity but, at the same time, the axial part heated decreases. The diameter of 500 μm was chosen as a compromise between heating as large an axial part as possible and keeping the two phases (reemission and collision) distinct and well separated. Of interest here is the reemission phase since it represents the emission of the wall after it is heated by the x-ray

source and the circulating flux inside the cylindrical cavity. The information contained in the experimental data set delivered by the two diagnostics (TGS and XRSC) has been unfolded to obtain the time integrated spectrum and the corresponding reemission phase radiation temperature from each axial location of the slit. In general lines, the procedure employed [19] to analyze the data is as follows: For a given axial distance from the source, the total amount of radiant energy density e_{tot} emitted during both the reemission and the collision phase is obtained (in absolute numbers) by wavelength integration of the TGS spectra. The XRSC data are used, on the other hand, to deduce the fraction a_r of the energy density emitted during the reemission phase to the total radiant energy density and its duration τ_r. Using this information, the radiation temperature profile for the reemission phase is determined from the Stefan-Boltzmann law, i.e., $\sigma T_r^4 = a_r e_{tot}/\tau_r$. The results from the analysis of several shots for selected axial locations from both types of targets are depicted in Fig. 3.

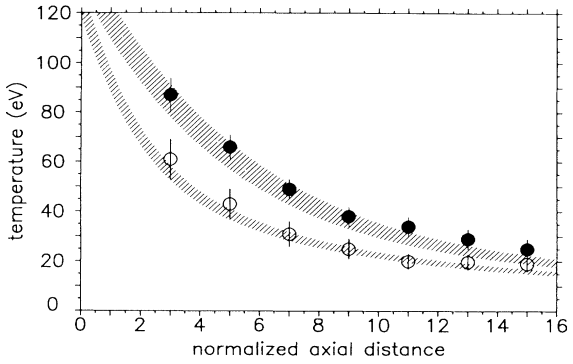

FIG. 3. Comparison of the experimentally obtained reemission phase radiation temperature profile (points) with the predictions of the theoretical model (hatched area) for a source temperature of $T_0 = 154 \pm 7$ eV and for a heating period of $t = 675 \pm 75$ ps. The full circles represent the closed geometry case while the empty circles represent the open one. The axial distance is normalized to the radius. The error bars correspond to the statistical error as determined from three shots. The hatched area indicates the uncertainty in the theoretical prediction resulting from the variation of the source radiation temperature and pulse duration.

The main effect of the reemission and of the resulting energy redistribution is the increase of the temperature at a given axial distance. Every wall element reemits energy and hence contributes to the heating of wall elements closer to but also farther away from the source. In the open geometry targets, the effect of the reemission is greatly suppressed since most of the cylindrical wall is missing. The radiation temperature of the remaining wall elements corresponds then to the direct heating by the source only. As can be seen in Fig. 3, the radiatively redistributed energy in a closed geometry target results in a quite pronounced increase in radiation temperature compared to an open geometry target over the whole axial distance. As expected, the maximum difference in temperature is in the vicinity of the source (at ≈ 3–7 radii axial distance) where, in terms of the reemitted flux, it amounts to a factor of 4–6.

As discussed in detail in Ref. [8], the reemitted flux $S_r(\hat{z},t)$ in a cylindrical cavity of radius r_0 and of normalized length $\hat{l} = l/r_0$ at a normalized distance $\hat{z} = z/r_0$ from the source and after a heating period t is given as the solution to the following implicit equation:

$$S_r(\hat{z},t) = ct^{\alpha}\left[\frac{S_0}{\pi}G(\hat{z}) + \int_0^{\hat{l}} \frac{S_r(\hat{z}',t)}{\pi} F(\hat{z},\hat{z}')d\hat{z}' - S_r(\hat{z},t)\right]^{\beta}. \quad (1)$$

In this equation, the radiant exchange process is described by two view factors associated with the cylindrical geometry: the view factor $G(\hat{z})$ between the source and a point on the cylindrical surface and the view factor $F(\hat{z},\hat{z}')$ between two points of the cylindrical surface [8]. The constant c and the exponents α,β are related to the physical properties of the wall material (equation of state, opacities). The source flux S_0 is related to the radiation temperature of the source T_0 through the Stefan-Boltzmann relation $S_0 = \sigma T_0^4$. The first term on the right-hand side of Eq. (1) represents the contribution of the source to the incident flux at a distance $\hat{z}$ while the integral in the second term represents the total contribution from all other wall elements along the cylindrical cavity. The model assumes a heating pulse that is constant in time and, therefore, the realistic case with a finite rise and falling time pulse cannot be simulated in detail. In view of this limitation, it was deemed appropriate to convert the experimentally measured heating pulse from the source into a flat-top with the same amplitude and energy content. The values obtained in this way were used as input parameters to the model. The solution of Eq. (1) for input parameters corresponding to the experimental conditions $T_0 = 154 \pm 7$ eV, $t = 675 \pm 75$ ps, $\hat{l} = 40$ and the values of the constants c,α,β for gold [8] are shown in Fig. 3 along with the experimental data. The open geometry case is easily simulated by setting the view factor $F(\hat{z},\hat{z}') = 0$. The temperature profile is obtained from the reemitted flux $S_r(\hat{z},t)$ using the Stefan-Boltzmann relation. In this model the finite speed of light has been disregarded. According to the theory of pure photon diffusion (random walk) in a cylindrical channel [22], at each moment t there is a heated region with characteristic length $z_D \sim (2r_0 ct)^{1/2}$. For $r_0 = 250$ μm and for the heating period of the source one obtains $z_D \approx 1.0$ cm.

Since this axial length is considerably larger than the observed length of ~ 0.5 cm (see Fig. 2), it is legitimate to neglect effects due to the finite speed of light.

In summary, the experimental data presented clearly show redistribution of energy occurring in a closed geometry x-ray heated cylindrical cavity. Furthermore, within experimental accuracy good agreement (over 2 orders of magnitude in flux) between theoretical prediction and experimental results for both types of targets leads us to conclude that the multiple absorption-reemission process is indeed responsible for this radiative energy redistribution. Hence, it constitutes a confirmation for the concept of radiation confinement and isotropization due to reemission which, using the same material data, has previously led to satisfactory modeling of the average temperature in spherical cavities [23]. It also indicates that the theoretical model described in Ref. [8] accurately reflects the physics of radiatively heated wall elements and of the energy exchange via radiation in the experimentally interesting flux region of $\sim 10^{13}$–10^{14} W/cm^2 ($T_0 \simeq 100$–180 eV). Since this formalism can easily be extended to three dimensions, it may be employed as an expedient tool to cavity optimization studies thus avoiding complicated and expensive simulation codes.

The authors are thankful to H. Baumhacker, G. Brederlow, F. Denk, and G. Keller for the operation of the laser facility. They would like also to express their appreciation to R. Sigel, S. Witkowski, and K. Eidmann for reading the manuscript and making useful suggestions. This work was supported in part by the Commission of the European Communities in the framework of the Association Euratom-Max-Planck-Institut für Plasmaphysik.

[1] R. L. McCrory and C. P. Verdon, in *Inertial Confinement Fusion*, Proceedings of the Course and Workshop of the International School of Physics Piero Caldirola, Varenna, September 1988, edited by A. Caruso and E. Sindoni (Editrice Compositori, Bologna, 1989), p. 183.
[2] S. Atzeni, Europhys. Lett. **11**, 639 (1990).
[3] Y. Kato *et al.*, Phys. Rev. Lett. **53**, 1057 (1984).
[4] S. P. Obenschein *et al.*, Phys. Rev. Lett. **56**, 2807 (1986).
[5] S. Skupsky *et al.*, J. Appl. Phys. **66**, 3456 (1989).
[6] E. Storm, J. Fusion Energy **7**, 131 (1988).
[7] R. Pakula and R. Sigel, Z. Naturforsch. **41a**, 463 (1986).
[8] G. D. Tsakiris, Phys. Fluids B **4**, 992 (1992).
[9] R. Pakula and R. Sigel, Phys. Fluids **28**, 232 (1985); **29**, 1340E (1986).
[10] G. D. Tsakiris *et al.*, Europhys. Lett. **2**, 213 (1986).
[11] S. Sakabe *et al.*, Phys. Rev. A **38**, 5756 (1988).
[12] R. Sigel *et al.*, Phys. Rev. Lett. **65**, 587 (1990).
[13] G. D. Tsakiris *et al.*, Phys. Rev. A **42**, 6188 (1990).
[14] Y. Kato *et al.*, Nucl. Fusion Suppl. **3**, 89 (1991).
[15] B. A. Remington *et al.*, Phys. Rev. Lett. **67**, 3259 (1991); B. A. Remington *et al.*, Phys. Fluids B **4**, 967 (1992).
[16] G. Brederlow, E. Fill, and K. J. Witte, *The High-Power Iodine Laser* (Springer, Berlin, 1983).
[17] K. Eidmann *et al.*, Laser Part. Beams **4**, 521 (1986).
[18] G. D. Tsakiris, Proc. SPIE Int. Soc. Opt. Eng. **1032**, 910 (1989).
[19] C. Stöckl, Ph.D. dissertation, Technische Hochschule Darmstadt, Darmstadt, 1992 (unpublished).
[20] P. Celliers and K. Eidmann, Phys. Rev. A **41**, 3270 (1990).
[21] C. Stöckl and G. D. Tsakiris, Laser Part. Beams **9**, 725 (1991).
[22] I. B. Kosarev *et al.*, Dokl. Akad. Nauk SSSR **206**, 572 (1973) [Sov. Phys. Dokl. **17**, 886 (1973)].
[23] R. Sigel *et al.*, Nucl. Fusion Suppl. **3**, 81 (1991).

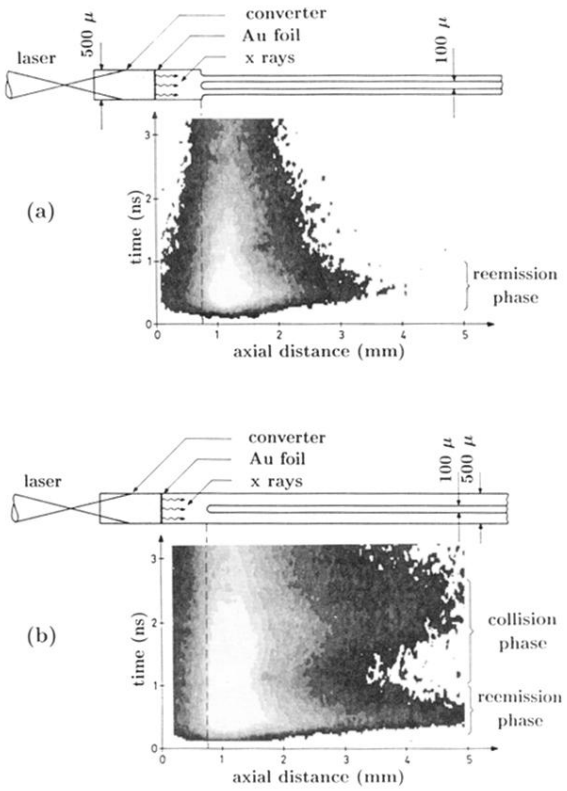

FIG. 2. Isointensity representation of the temporal evolution of the radiation emanating from the diagnostic slit of the (a) open and (b) closed geometry targets.